Check for updates

Numerical analysis of optical vortices generation with nanostructured phase masks

HUE THI NGUYEN,[1,2] ALICJA ANUSZKIEWICZ,[1,3,*] JOLANTA LISOWSKA,[1,2] ADAM FILIPKOWSKI,[1,2] RAFAL KASZTELANIC,[1,2] RYSZARD BUCZYNSKI,[1,2] AND WIESLAW KROLIKOWSKI[4,5]

[1]*Department of Glass, Lukasiewicz Research Network - Institute of Electronic Materials Technology, Wolczynska 133, 01-919 Warsaw, Poland*
[2]*Faculty of Physics, University of Warsaw, Pasteura 5, 02-093 Warsaw, Poland*
[3]*Faculty of Electronics and Information Technology, Institute of Electronic Systems, Warsaw University of Technology, Nowowiejska 15/19, 00-665 Warsaw, Poland*
[4]*Science Program, Texas A&M University at Qatar, Doha, Qatar*
[5]*Laser Physics Centre, Research School of Physics, Australian National University, Canberra, ACT 0200, Australia*
[*]*alicja.anuszkiewicz@itme.edu.pl*

Abstract: We study the theoretical formation of optical vortices using a nanostructured gradient index phase mask. We consider structures composed of spatially distributed thermally matched glass nanorods with high and low refractive indices. Influence of effective refractive profile distribution, refractive index contrast of component glasses and charge value on the quality of generation of vortices are discussed. A trade-off between waveguiding and phase modulation effects for various refractive index contrast is presented and analysed.

1. Introduction

The continuous interest in optical vortices (OV) is stimulated by their broad application potential which includes, among others, optical tweezers for particle or cell manipulation [1], phase contrast microscopy for enhancement of imaging resolution [2] or laser micromachining for fabrication of surface and bulk structures in metals or semiconductors [3].

There are several common methods to generate vortex beams. They involve use through spiral phase-plate (SPP) [4], computer generated holograms [5], spatial light modulators (SLMs) [6] or spiral mirrors [7]. Transmission, diffraction or reflection of fundamental light beams from these optical elements converts them into optical vortices. These vortices are typically of macroscopic spatial dimension. However, for application in compact fiber-based optics, small size vortices, and consequently their micron-size converters are particularly relevant as they can be directly integrated with optical fiber optics. Few recent works have demonstrated fabrication of microscopic size spiral phase plates by using 2-photon absorption mediated 3D direct laser writing [8] or by electron beam lithography [9]. 3D-printing has been recently employed to create vortex converter directly at the tip of an optical fiber [10]. All the methods have particular advantages and limitations, which is, for instance, a result of geometry or refractive index value and dispersion, i.e. traditional spiral phase plate very often needs index-matching immersion to produce an optical vortex with low topological charge [11]. Spatial light modulators give a possibility to dynamic change the phase distribution, but are expensive, relatively large, and have limited power for input beam and limited spatial and phase resolution. The 3D laser written SPPs are very small (40 μm in diameter) and can be produced directly on the optical fiber tip, but because of reduced writing laser beam resolution, this kind of SPP is staircase, not continuous and limit input power of the beam [8]. Moreover, the 3D writing is based on system utilising the

principle of two-photon absorption, which is quite expensive, as it is also in the case of electron beam lithography system [9].

We have recently proposed a new approach for fabrication of transmission gradient index vortex masks using standard low-cost fiber drawing stack-and-draw technique [12]. An arbitrary refractive index distribution is obtained via formation of internal index nanostructure composed of two types of low and high index nanorods arranged in a hexagonal lattice. Because of their subwavelength transverse size, they constitute the so called nanostructured gradient index (nGRIN) materials with a local averaged refractive index determined by the effective medium theory (e.g. Maxwell-Garnett approach) [13]. This spatial structuring approach proved to be very successful in development of various all-glass compact (around 20-40 μm in diameter) components with broad functionalities [14–17], in a form of parallel plates, that can be easily integrated with other micro-optical components and, in particular, optical fibers [18].

Our recent work presented the proof-of-concept vortex nanostructured phase mask [12]. We have shown that the phase mask indeed converts fundamental (Gaussian) beam into an optical vortex with azimuthal phase distribution, which can be optimised to work at dedicated wavelength and vortex charge. However, we also observed in experiments that while the mask provided correct helical phase structure, the generated vortex exhibited azimuthally non-uniform intensity distribution with intensity maximum forming in the area of highest value of refractive index. This phenomenon is highly disadvantageous since limits practical application of the proposed nanostructured phase masks, where highly uniform intensity distribution in vortex beam is required, as in case of particle trapping [19] or surface structuration [20].

In this work we study the influence of refractive index distribution in the nanostructured mask, on generation of fundamental as well as higher charge vortex beams. In particular, we consider various azimuthal profiles of refractive index distribution. As the gradient masks can be fabricated by using various pairs of low and high index glasses, they can have different gradient coefficient and thickness. We study the influence of glass refractive index on intensity and phase distribution in generated vortex beam. Based on numerical analysis, we validate a potential of newly proposed method for development of gradient index vortex masks.

2. Vortex beam generation with nanostructured phase-mask and spiral phase-plate: a comparison

The unique fabrication capabilities of nanostructuring technique have been confirmed by demonstration of numerous index gradient-based optical components including, e.g. nGRIN lenses [14,15], nGRIN axicons [16] and nanostructured fibers with parabolic profile of refractive index in the core [21]. In particular, we have recently fabricated a flat-surface gradient (nGRIN) vortex masks [10] and demonstrated, for the first time, their suitability to convert an incident Gaussian beam into an optical vortex.

The main difference between the conventional transmission type spiral phase-plate (SPP) and our proposed nanostructured phase mask (NPM) is an origin of the phase modulation. In case of the former shown in Fig. 1(a) the required azimuthal phase distribution of the transmitted wave, the necessary total phase modulation $\Delta\varphi_{SPP}$ for vortex formation with the beam of wavelength λ, is achieved by azimuthal variation of local mask's thickness such that:

$$\Delta\varphi_{SPP} = \frac{2\pi h}{\lambda}(n_{SPP} - n_{air}) = \frac{2\pi h}{\lambda}(n_{SPP} - 1),\qquad(1)$$

where h represents the step in mask thickness as indicated in Fig. 1(a). In our novel approach depicted in Fig. 1(b), the thickness of the mask d is fixed, and the desired angular phase variation is obtained by introducing azimuthal effective index gradient giving:

$$\Delta\varphi_{NPM} = \frac{2\pi d}{\lambda}(n_{high} - n_{low}).\qquad(2)$$

In both formulas, (n_{SPP}–1) and (n_{high}–n_{low}) are the refractive index contrasts (Δn) of respective spiral phase-plate and nanostructured phase mask. Topological charge of the generated vortex beam, m, is then determined by the total azimuthal phase change as:

$$\Delta \varphi_{SPP,NPM} = 2\pi m. \tag{3}$$

As the relations Eq. (1) and Eq. (2), are wavelength-dependent, performance of both types of phase-masks depends on refractive index dispersions. In the case of SPP the refractive index contrast is high, as e.g. for typical BK7 glass [14] it equals to 0.5 at 1.55 μm and it only depends on dispersion of base glass as the air dispersion is negligible. Because of high Δn, it is rather difficult to generate vortices with low topological charges. To decrease the index contrast index matching fluid must be used. On the other hand, properties of the NPM are determined by the dispersion of both base glasses, and hence this design offers an additional degree of freedom in optimization of the fabricated components. One can choose the index contrast such that it will allow to create vortex of desired charge for practically feasible thickness.
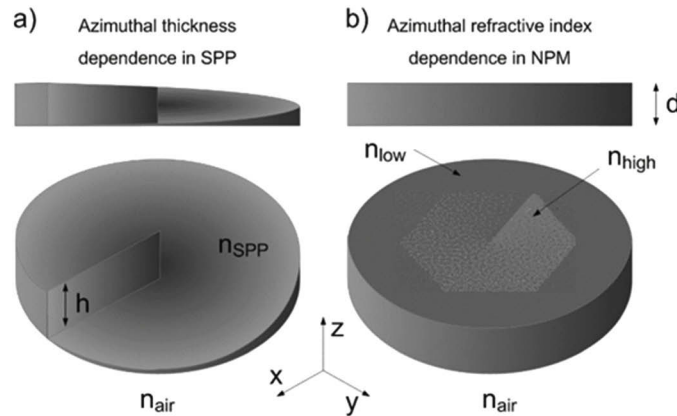

Fig. 1. Schematic comparison between spiral phase-plate (SPP) (a) and nanostructured phase-mask (NPM) (b).

3. Methods of modelling of nanostructured phase mask

Our earlier experiments with fabricated flat nanostructured vortex mask showed undesired phenomenon of vortex deformation. Although the beam transmitted through mask acquired donut-like shape and had correct helical phase structure, the light intensity distribution was azimuthally non-uniform exhibiting clear tendency for localization in the high index region of
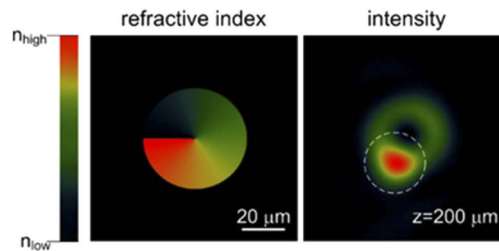

Fig. 2. Generation of vortex beam with gradient index phase mask: azimuthal gradient index distribution (a), profile of azimuthal refractive index distribution (b).

the mask. This is particularly evident in thick masks involving longer distance light propagation. This vortex deformation is illustrated in Fig. 2, which shows numerically calculated far field intensity and phase distribution of the beam transmitted by the vortex mask of thickness of 50 microns. The deformation of vortex structure may limit practical applicability of the transmission mask. Therefore, in the reminder of the paper, we will numerically investigate performance of the mask in vortex formation. In particular, we will explore possibility to improve the angular light intensity pattern by considering masks with various types of angular index profiles.

To model a performance of NPM we used Fourier Transform-based Beam Propagation Method (BPM). In this method in homogeneous medium with the refractive index $\bar{n}$ free space propagation of the beam ψ_{fs} by the small distance s can be described by complex field [22]:

$$\psi_{fs}(x, y, z + s) = F^{-1}\{F\{\psi_{fs}(x, y, z)\} \exp(-i\beta s)\}, \tag{4}$$

where F is the Fourier transform and:

$$\beta^2 = k_0^2 n_0^2 - 4\pi^2(v_x^2 + v_y^2). \tag{5}$$

In our case the medium in which beam is propagating is inhomogeneous with refractive index distribution $n(x,y)$, therefore the phase correction must be applied [22]:

$$\psi(x, y, z + s) = \exp[-ik_0(n - \bar{n})s]\psi_{fs}(x, y, z + s). \tag{6}$$

The correction may be applied in simplified form only if both s and $n - \bar{n}$ are sufficiently small [22]. One can utilize the described procedure for the numerical computation of the complex field at $\psi(x,y,z_i)$ in the subsequent planes perpendicular to Z axis if the initial field for z_0 is known.

In our simulations we assume a source planar input beam with wavelength of 1.55 μm and with Gaussian intensity distribution limited by circular aperture with diameter of 20 μm. All investigated vortex masks were 50 μm in diameter, and for simplicity, we assumed their continuous refractive index changing from n_{high} to n_{low} with corresponding thickness d. n_{high} and n_{low} denote refractive indices of high and low index glasses used to form NPM.

Our studies of possible modification of the NPMs to improve uniformity of generated vortex beams concentrate on:

- an influence of refractive index contrast in NPM with charge 1;

- an influence of azimuthal refractive index distribution profile in NPM with charge 1;

- an influence of number of phase periods in NPM, for high charge vortex generation.

4. Influence of refractive index contrast in gradient index mask on vortex generation

The NPMs are developed with two types of glass nanorods. The selection of glasses determines refractive index contrast achieved in the vortex mask and its thickness for NPM with topological charge 1. Numerical simulations are performed for 3 selected cases for pairs of glasses with various contrast of refractive index. Material dispersion of selected glasses is shown in Fig. 3. We emphasize that we consider only real, developed and experimentally characterised glass materials. We additionally limited selected materials to the pairs of thermally matched glasses, to ensure successful fabrication of NPMs. The selected glasses pairs were previously verified experimentally for joint thermally processing in fiber drawing tower [16,21,23], and include:

a) fused silica glass based structure composed of fused silica (FS) and 4.9%mol Ge-doped silica nanorods. This structure has relatively low refractive index contrast Δn ≈ 0.007 that corresponds to NPM with charge +1 with thickness of 230 μm. The structure is labelled as FS;

b) silicate glass based structure composed of nanorods made of two in-house synthesized borosilicate glasses labelled as NC21 and NC32. The borosilicate glasses NC21 and NC32 have a different content of BaO, Na_2O and K_2O in their composition, which results in difference in their material dispersion [24]. This structure has moderate refractive index contrast $\Delta n \approx 0.025$ that corresponds to NPM with charge +1 with thickness of 60 µm. The structure is labelled as NC;

c) soft glass based structure composed of nanorods made of two in-house synthesized glasses: lead-bismuth-gallate glass PBG81 and thermally matched silicate glass UV710 [23]. This structure has very high refractive index contrast $\Delta n \approx 0.376$ that corresponds to NPM with charge +1 with thickness of 4 µm. The structure is labelled as UP.
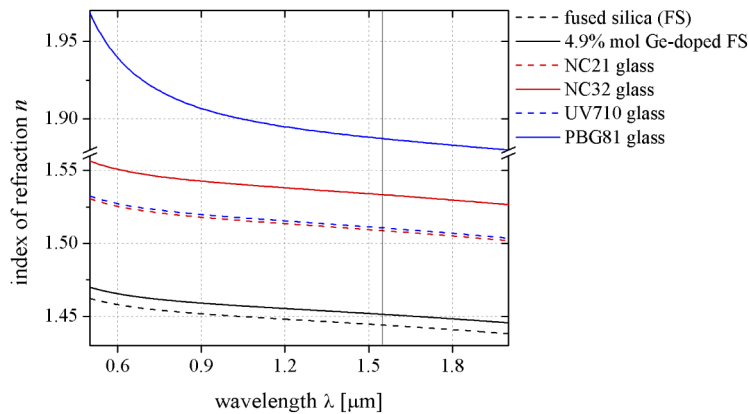

Fig. 3. Material dispersion for three pairs of glasses selected for development of NPM.

The refractive index contrasts for the selected three pairs of glasses define the structure thickness accordingly to the Eq. (2). Assuming the optical vortex with charge $m=1$, such that $\Delta\varphi_{NPM}=2\pi$ at $\lambda=1.55$ µm, and linear azimuthal refractive index distribution, we obtain three structures of different thicknesses (Table 1).

Table 1. Fundamental properties of investigated structures.

Structure name	Glass type	Refractive index at 1.55 µm	Refractive index contrast between glasses at 1.55 µm Δn	Thickness of nanostructured phase mask with charge 1 d [µm]
FS	Fused silica	1.444	0.007	230
	4.9%mol Ge-doped FS	1.451		
NC	NC21	1.509	0.025	60
	NC32	1.533		
UP	UV710	1.511	0.376	4
	PBG81	1.887		

The structures FS, NC and UP with appropriate thickness d were implemented in the numerical model as continuous gradient structures and their abilities in generation of optical vortex were analysed. The simulation steps along x and y directions were 0.1 µm in the structures as well as in free space. The steps along the z axis inside the structure and in the free space were 0.1 µm and 0.5 µm, respectively. Depending on the structure, there is certain distance along which the

vortex distribution builds up. Therefore, we selected the common distance of 200 μm from the NPM output surface to visualize the results, as shown in Fig. 4. All images for refractive index and intensity distribution correspond to the simulation area of 150×150 μm. For the phase, the images are restricted to 50×50 μm region.
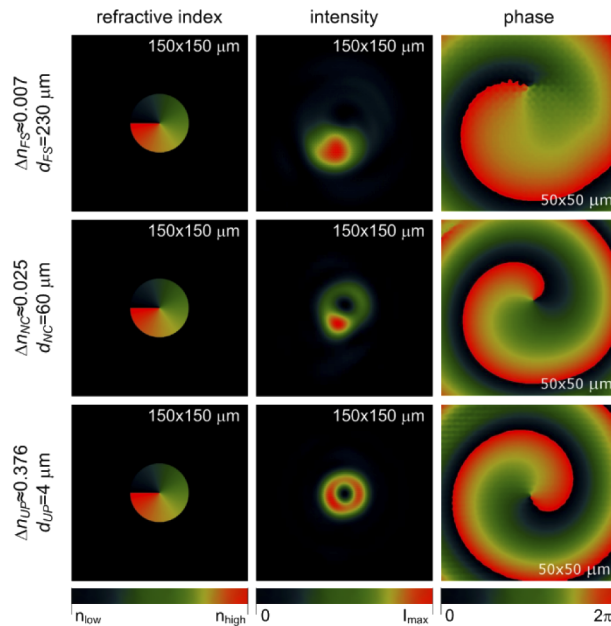

Fig. 4. Refractive index, intensity and phase distribution (columns) calculated for three types of vortex masks (rows). The rows represent the FS, NC and UP structures, respectively.

The results obtained for FS structure show detrimental light localization caused by a waveguiding effect that occurs in high refractive index area of NPM. This is particularly evident for long distance light propagation, i.e. for thick vortex mask (230 μm). The light localization is strong and expected donut intensity distribution is hardly visible. On the other hand, the singular vortex phase distribution is still maintained. However, position of phase singularity is slightly shifted (~10 μm) from the center of the structure toward the high intensity spot. This behaviour basically disqualifies the FS structures as far as its practical application is concerned, and hence will not be discussed further.

For the NC structure, which has a smaller thickness for the charge $m=1$ (60 μm), the intensity distribution is more uniform. The donut intensity profile is visible and the singularity of phase distribution matches the center of the structure. Nevertheless, the intensity distribution is still azimuthally non-uniform as we observe formation of high intensity spot related to high refractive index area of NPM and the waveguiding effect.

The best result was obtained for UP structure with highest refractive index contrast and smallest thickness (4 μm), which can be treated as purely phase component with negligible thickness. The donut shape intensity distribution is uniform and singularity of phase profile matches perfectly the center of the mask.

This numerical result has shown that waveguiding effect that exists in gradient index vortex masks depends strongly on their thickness. For longer masks we observe strong localization of light in the area of high refractive index. Although their phase distribution is still correct, the non-uniform azimuthal intensity distribution limit their practical application. We see clearly that a reduction of mask thickness ensures the best quality of generated vortex beam. Therefore, development of very thin NPM with high refractive index contrast is strongly desired. However,

the fabrication of such a thin, few micrometers thick component is challenging from technological point of view, since the NPMs are fabricated (in the final step) by grinding and polishing. It is difficult to control these mechanical processes with accuracy of fraction of micrometer. As alternative approach, chemical etching processes [25,26] could be employed to fabricate thin mask.

5. Influence of azimuthal refractive index distribution profile in gradient index mask on vortex generation

As we showed above, a high quality of vortex beam with charge 1 with uniform azimuthal intensity distribution can be obtained only for very thin gradient index phase masks. However, the masks studied in previous section exhibited linear azimuthal refractive index dependence. In this section we explore the effect of azimuthal nonlinear modification of gradient index profile on the quality of vortex formation. We consider the NPMs with various thickness and non-uniform azimuthal refractive index profiles. We model the angular index profile using the following relation:

$$n(\alpha) = n_{low} + \Delta n \left(\frac{\alpha}{2\pi} \right)^{\frac{1}{g}}, \tag{7}$$

where α is azimuthal angle ($0 < \alpha < 2\pi$), g is the shape power index, and Δn denotes refractive index contrast defined as:

$$\Delta n = n_{high} - n_{low}, \tag{8}$$

where n_{high} and n_{low} denote refractive indices of high and low refractive index glasses.

The shape power index g determines azimuthal refractive index distribution (Fig. 5). For large g values, i.e. $g=4$, the area of high refractive index in the NPM is extended, while for its fractional value, i.e. $g=1/16$, the high refractive index area is minimized (Fig. 6).
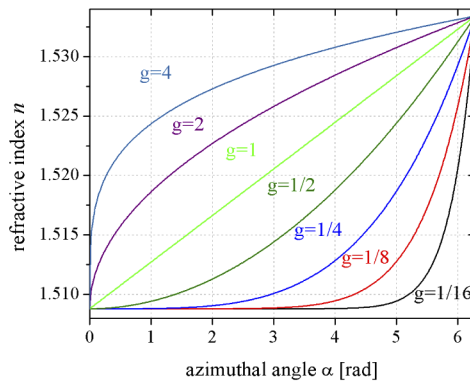
Fig. 5. Refractive index profile as a function of azimuthal angle for NC structure of gradient index phase mask with thickness of 60 μm for various values of the shape power index g defined in Eq. (7).

Vortex beams generated by NPMs with various azimuthal profiles for NC structure are presented in Fig. 6. Intensity distribution in the donut beam clearly depends on shape power index g. In case of structures with a large g, intensity is highly non-uniform and strongly localised in single spot. Similar effect occurs for low values of the shape power index below $g=1/4$. In the range between, e.g. $g=1/4$ and $g=1$ the light is more uniformly distributed in the ring but localization spot is still clearly visible. The phase distributions are satisfactory for most of the structures, however for $g=1/8$ and $g=1/16$ the optical vortex properties are not preserved anymore, as the phase singularity is lost resulting in appearance of centrally located region of
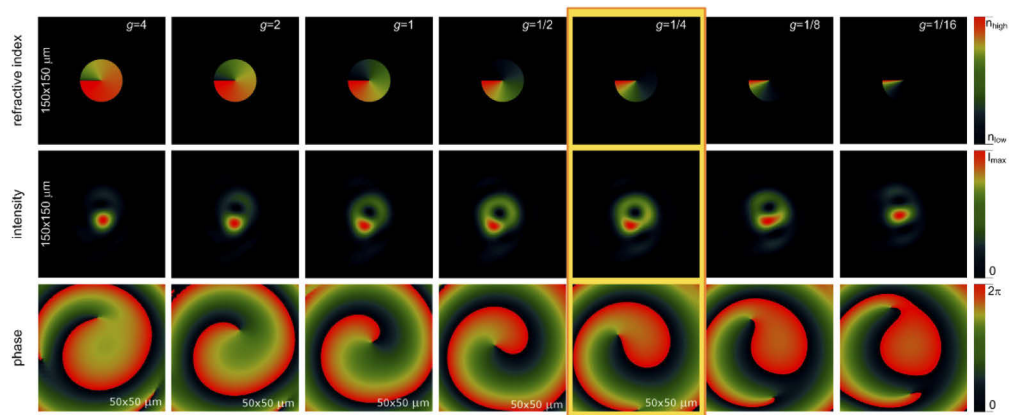
Fig. 6. Generation of vortex beam with gradient index phase mask with various azimuthal refractive index profiles determined by shape power index g. A NC gradient index phase mask with thickness of $60\,\mu m$, that corresponds to 2π phase shift is considered.

constant phase. The best results are obtained for $g=1/4$ (highlighted frame in Fig. 6). In that case, while light waveguiding still exists, its detrimental effect is drastically reduced leading to the formation of acceptable quality microscopic-size vortex beam. It is important that this is achieved with moderate refractive index contrast and, at the same time, ensures feasible thickness of the mask. Indeed, the NPM structure with thickness of $60\,\mu m$, which corresponds to charge $m=1$ is relatively easy to develop with standard mechanical gridding and polishing processes as we shown previously [16].

Next, we conducted series of simulations representing vortex formation in gradient index phase masks UP with large refractive index contrast of $\Delta n \approx 0.376$ and small thickness of the mask ($4\,\mu m$). Results of these simulations are presented in Fig. 7. It turns out, that the optimum phase distribution as well as uniform intensity distribution in donut beam is obtained for the mask with linear profile of azimuthal refractive index distribution ($g=1$). Any departure from $g=1$ has detrimental effect on vortex quality by leading to the appearance of localised strong intensity region.
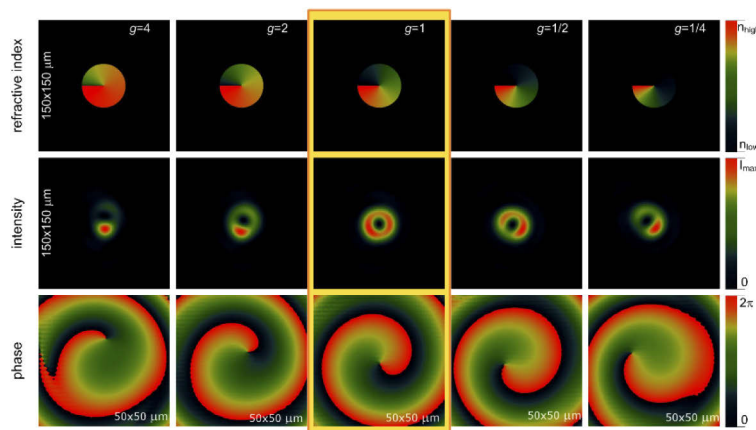

Fig. 7. Generation of vortex beam with gradient index phase mask with various azimuthal refractive index profiles determined by the shape power index g. An UP gradient index phase mask with thickness of $4\,\mu m$, that corresponds to 2π phase shift is considered.

Our results in this section show that the use of nonlinear monotonic azimuthal refractive index profile is good solution for thick NPM, e.g. NC structure. It allows one to compensate for the waveguiding effect that is responsible for light localization in the area of highest refractive index, preserving, at the same time, the phase singularity. Furthermore, optimum profile of refractive index depends mainly on refractive index contrast in NPMs and has to be individually selected for every type of NPMs.

6. Generation of high charge vortices with nanostructured masks – the role of high index gradient

Until now we have been considering generation of single charge vortices which require only 2π total angular phase shift. To generate vortices of charge larger than 1, the multiple of 2π phase shift must be achieved. The simple increase mask's thickness by factor of 2 or higher will not work since it would enhance the waveguiding effect as discussed in previous section. On the other hand, keeping the thickness of the mask constant would require finding materials with higher index contrast, which is practically not feasible. The only real option then is to maintain the thickness of the mask and the two constitute glasses unchanged (as for vortex with the charge m=1), but divide the mask into a number of identical angular zones, with the phase change of 2π in each zone. This technique has been successfully implemented in reflective vortex masks [7], where generation of vortices with charge of the order of thousands was demonstrated. The principle of this approach employed to our nanostructured mask is illustrated in Fig. 8. The plots depict required index profiles (here with constant gradient) to create multiple 2π phase profiles for the wavelength of 1.55 μm. We consider here the 4 μm -thick constant gradient index phase masks with diameter of 50 μm and with 1, 2, 3, 4, 5, 6 and 9 2π-phase steps distributed uniformly clockwise, which should generate the optical vortex with the charge m= +1, +2, +3, +4, +5, +6 and +9, respectively.
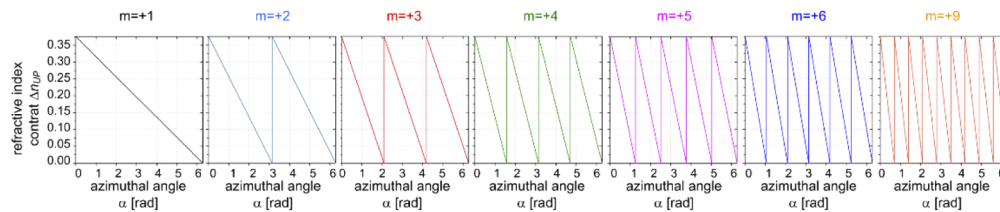

Fig. 8. Azimuthal linear index distribution that corresponds to single and multiple 2π-phase change for optical vortex generation with charge m=+1, +2, +3, +4, +5, +6, and +9 for the wavelength of 1.55 μm. An UP gradient index phase mask with thickness of 4 μm, that corresponds to 2π-phase shift is considered.

Vortex beams generated by NPM with various azimuthal profiles for UP structure are presented in Fig. 9. Vortex beams are successfully generated with 2π, 4π and 6π gradient index mask. In this case intensity distribution in the vortex beams is reasonably uniform and their phase profiles clearly indicate vortex beam with charges m=+1, m=+2 and m=+3, respectively. The intensity distributions are slightly affected by light localisation effect and the number of spots corresponds to the charge of vortex, which was also observed by other research groups in case of standard phase masks [27]. It is worth to note that two and three singularities can be distinguished in phase distributions of 4π and 6π gradient index masks respectively.

The output beams generated with 8π and higher gradient index masks are not vortex beam anymore. Their intensity distributions have donut shape with additional light localization in the center. In addition they have complex phase structure with flat phase in the center and vortex-like phase distribution in peripheral areas.
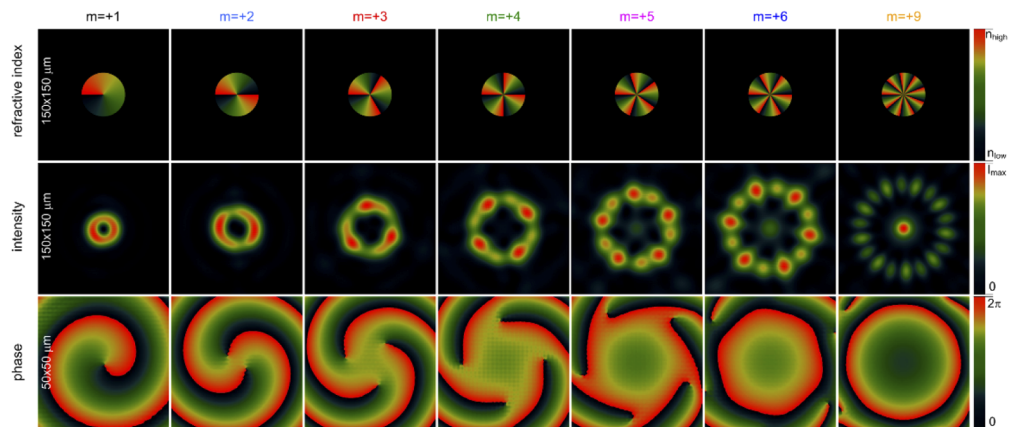
Fig. 9. Generation of vortex beam with topological charge of *m*=+1, +2, +3, +4, +5, +6, and +9 with gradient index phase mask with various multiple 2π phase change azimuthal refractive index profiles. An UP gradient index phase mask with thickness of 4 μm, that corresponds to 2π phase shift is considered.

The multiple singularities generated by 4π and 6π gradient index masks as well as destroying of vortex beam for higher than 6π gradient structures is related to the small size of the angular zones and sensitivity of high charge vortices to perturbation. In fact, these vortices can be destabilized breaking up into constituent single charge vortices. With increase of charge the size of individual 2π gradient zone becomes small enough that beam locally interacts simultaneously with multiple gradient structure. As a result, the averaging effect related to effective medium approximation [13] begins to play a dominant role in the centre of the generated beam with the NPM, where the individual 2π gradient zone has the area similar to wavelength. As a result central area with constant phase appears and the phase singularity is lost. For NPM with higher charges this effect is dominant for larger part of local medium and results in location of intensity peak in the centre of the beam.

The other way to obtain high-order vortices is to use a longer section of NPM with single charge *m*=+1, whose length corresponds to multiple 2π phase shift. In this case we consider only NPM composed of UP pairs of glasses with high difference of refractive indices. As we
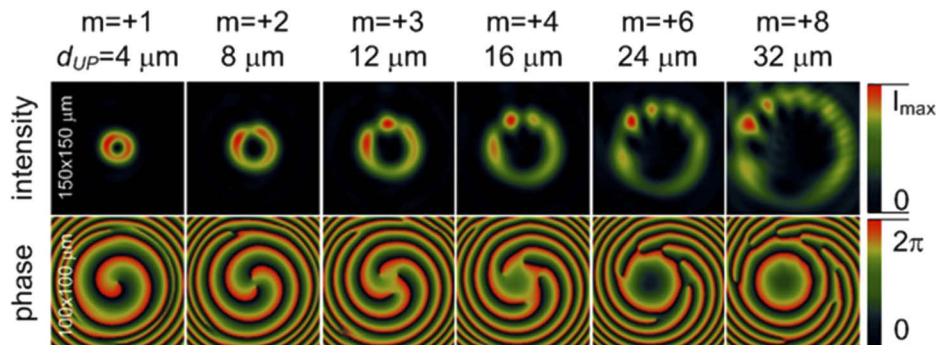

Fig. 10. Generation of vortex beam with topological charge of *m*=+1, +2, +3, +4, +5, +6, and +8 with linear gradient index phase mask with 2π phase change azimuthal refractive index profiles. An UP gradient index phase mask with various thickness, that corresponds to multiple 2π phase shift is considered.

have shown in Section 5 only use of UP pair of glasses allow to mitigate the waveguiding effect. We have performed series of simulation to verify performance of vortices with charge $m=+1$ to $m=+8$ (Fig. 10). The thickness of NMP vary form 4 till 32 μm.

A donut shape of intensity distribution is maintained without intensity spot in the center of the beam for all considered NPMs. As expected, due to increase of thickness the waveguiding effect exists and it can be observed in form of non-uniform intensity distributions in donut ring. A constant phase spot appears in the center of the beam for thicker NMPs, since high order singularity splits into fundamental ones that shift away from the beam center.

7. Conclusions

We studied here the performance of nanostructured gradient index phase masks in generation of optical vortices. Such masks suffer from the waveguiding effects which leads to azimuthally non-uniform light intensity distribution in generated singular beam. We demonstrated that the best approach to minimize this detrimental effect is to fabricate mask employing glasses which provide high index contrast. In that case the thickness of the mask can be made small so the waveguiding effect could be negligible and the only relevant process is spatial modulation of phase of incoming beam. We found that practically feasible vortex mask with charge $m=1$ can be created using in-house synthesized thermally matched pair of lead-bismuth-gallate glass PBG81 and silicate glass UV710. Since refractive index difference between the glasses is very high $\Delta n_{UP} \approx 0.376$, a phase mask with linear azimuthal gradient index profile that corresponds to 2π phase shift can be achieved in a plate of 4 μm thickness for the wavelength of 1.55 μm. This confirms that the NPM should be as thin as possible to behave as phase-only optical component. However, fabrication of such a thin components is technologically challenging due to requirements on thickness accuracy. Therefore, we proposed to fabricate masks with technically achievable thickness of 60 μm but employing instead of traditional linear, a non-uniform angular phase gradient (or equivalently index distribution). We demonstrated numerically significant improvement in uniformity of vortex light intensity distribution (and proper singular phase) by using nonlinear azimuthal gradient index function with the shape power index $g = 1/4$. In this case the index gradient grows slowly for small azimuthal angle and speeds up only when approaching 2π. As a result a 60 μm thick gradient index phase mask can be obtained if a pair of thermally matched borosilicate glasses NC21 and NC32 with moderate refractive index difference of $\Delta n_{NC} \approx 0.025$ are used for development of nanostructured gradient index phase mask. Our simulations showed that while waveguiding effect cannot be eliminated its effect can be minimized by proper selection of refractive index gradient function leading to a reasonable intensity pattern in the generated vortex.

We have also investigated possibility to use our nanostructured phase masks to generate vortices with high topological charge. To this end we considered masks consisting of multiple identical segments with total phase variation of 2π in each segment. We were able to generate a reasonable vortex beam with charge up to $m=3$. However, generation of higher charge vortices were unsuccessful as light propagation resulted in loss of phase singularity and formation of structures with nonzero light intensity in the center.

Vortices with high topological charge can be successfully generated if longer section of NPM with single charge $m=+1$ is used. In this case length of NPM corresponds to multiple 2π. We obtain correct donut shape without intensity spot in the center of the beam for all considered vortices with high charges. Non-uniform intensity distribution is still present, however this effect is mitigated for structures composed of glasses with high difference of refractive indices.

Disclosures

The authors declare no conflicts of interest.

References

1. B. K. Singh, H. Nagar, Y. Roichman, and A. Arie, "Particle manipulation beyond the diffraction limit using structured super-oscillating light beams," Light: Sci. Appl. **6**(9), e17050 (2017).
2. S. Fürhapter, A. Jesacher, S. Bernet, and M. Ritsch-Marte, "Spiral phase contrast imaging in microscopy," Opt. Express **13**(3), 689–694 (2005).
3. J. J. J. Nivas, S. He, A. Rubano, A. Vecchione, D. Paparo, L. Marrucci, R. Bruzzese, and S. Amoruso, "Direct Femtosecond Laser Surface Structuring with Optical Vortex Beams Generated by a q-plate," Sci. Rep. **5**(1), 17929 (2015).
4. V. V. Kotlyar, A. A. Almazov, S. N. Khonina, V. A. Soifer, H. Elfstrom, and J. Turunen, "Generation of phase singularity through diffracting a plane or Gaussian beam by a spiral phase plate," J. Opt. Soc. Am. A **22**(5), 849–861 (2005).
5. N. R. Heckenberg, R. McDuff, C. P. Smith, and A. G. White, "Generation of optical phase singularities by computer-generated holograms," Opt. Lett. **17**(3), 221–223 (1992).
6. D. Ganic, X. Gan, M. Gu, M. Hain, S. Somalingam, S. Stankovic, and T. Tschudi, "Generation of doughnut laser beams by use of a liquid-crystal cell with a conversion efficiency near 100," Opt. Lett. **27**(15), 1351–1353 (2002).
7. G. Campbell, B. Hage, B. Buchler, and P. K. Lam, "Generation of high-order optical vortices using directly machined spiral phase mirrors," Appl. Opt. **51**(7), 873–876 (2012).
8. S. Lightman, R. Gvishi, G. Hurvitz, and A. Arie, "Shaping of light beams by 3D direct laser writing on facets of nonlinear crystals," Opt. Lett. **40**(19), 4460–4463 (2015).
9. M. Massari, G. Ruffato, M. Gintoli, F. Ricci, and F. Romanato, "Fabrication and characterization of high-quality spiral phase plates for optical applications," Appl. Opt. **54**(13), 4077–4083 (2015).
10. K. Weber, F. Hütt, S. Thiele, T. Gissibl, A. Herkommer, and H. Giessen, "Single mode fiber based delivery of OAM light by 3D direct laser writing," Opt. Express **25**(17), 19672–19679 (2017).
11. M. W. Beijersbergen, R. P. C. Coerwinkel, M. Kristiensen, and J. P. Woerdman, "Helical-wave front laser beams produced with a spiral phase plate," Opt. Commun. **112**(5-6), 321–327 (1994).
12. K. Switkowski, A. Anuszkiewicz, A. Filipkowski, D. Pysz, R. Stępień, W. Królikowski, and R. Buczynski, "Formation of optical vortices with all-glass nanostructured gradient index masks," Opt. Express **25**(25), 31443–31450 (2017).
13. A. Sihvola, *Electromagnetic Mixing Formulas and Applications*, (The Institution of Electrical Engineers, 1999).
14. J. Nowosielski, R. Buczynski, A. J. Waddie, A. Filipkowski, D. Pysz, A. McCarthy, R. Stepien, and M. R. Taghizadeh, "Large diameter nanostructured gradient index lens," Opt. Express **20**(11), 11767–11777 (2012).
15. R. Kasztelanic, A. Filipkowski, D. Pysz, R. Stepień, A. J. Waddie, M. R. Taghizadeh, and R. Buczynski, "High resolution Shack-Hartmann sensor based on array of nanostructured GRIN lenses," Opt. Express **25**(3), 1680–1691 (2017).
16. A. Filipkowski, B. Piechal, D. Pysz, R. Stepien, A. Waddie, M. R. Taghizadeh, and R. Buczynski, "Nanostructured gradient index microaxicons made by a modified stack and draw method," Opt. Lett. **40**(22), 5200–5203 (2015).
17. A. J. Waddie, R. Buczynski, F. Hudelist, J. Nowosielski, D. Pysz, R. Stepien, and M. R. Taghizadeh, "Form birefringence in nanostructured micro-optical devices," Opt. Mater. Express **1**(7), 1251–1261 (2011).
18. R. Kasztelanic, A. Filipkowski, A. Anuszkiewicz, P. Stafiej, G. Stepniewski, D. Pysz, K. Krzyżak, R. Stepien, M. Klimczak, and R. Buczynski, "Integrating Free-Form Nanostructured GRIN Microlenses with Single-Mode Fibers for Optofluidic Systems," Sci. Rep. **8**(1), 5072 (2018).
19. L. Gong, B. Gu, G. Rui, Y. Cui, Z. Zhu, and Q. Zhan, "Optical forces of focused femtosecond laser pulses on nonlinear optical Rayleigh particles," Photonics Res. **6**(2), 138–143 (2018).
20. T. Omatsu, K. Miyamoto, K. Toyoda, R. Morita, Y. Arita, and K. Dholakia, "A New Twist for Materials Science : The Formation of Chiral Structures using The Angular Momentum of Light," Adv. Opt. Mater. **7**(14), 1801672 (2019).
21. A. Anuszkiewicz, R. Kasztelanic, A. Filipkowski, G. Stepniewski, T. Stefaniuk, B. Siwicki, D. Pysz, M. Klimczak, and R. Buczynski, "Fused silica optical fibers with graded index nanostructured core," Sci. Rep. **8**(1), 12329 (2018).
22. K. Okamoto, "Fundamentals of Optical Waveguides," (Academic, San Diego, 2000).
23. J. Cimek, R. Stępień, G. Stepniewski, B. Siwicki, P. Stafiej, M. Klimczak, D. Pysz, and R. Buczyński, "High contrast glasses for all-solid fibers fabrication," Opt. Mater. **62**, 159–163 (2016).
24. R. Stępień, J. Cimek, D. Pysz, I. Kujawa, M. Klimczak, and R. Buczyński, "Soft glasses for photonic crystal fibers and microstructured optical components," Opt. Eng. **53**(7), 071815 (2014).
25. L. M. Cook, "Chemical processes in glass polishing," J. Non-Cryst. Solids **120**(1-3), 152–171 (1990).
26. G. Zhao, Z. Wei, W. Wang, D. Feng, A. Xu, W. Liu, and Z. Song, "Review on modeling and application of chemical mechanical polishing," Nanotechnol. Rev. **9**(1), 182–189 (2020).
27. J. Wang, A. Cao, M. Zhang, H. Pang, S. Hu, Y. Fu, L. Shi, and Q. Deng, "Study of characteristics of vortex beam produced by fabricated spiral phase plates," IEEE Photonics J. **8**(2), 1–9 (2016).